Visual Tactile Sensor based on Feature Tracking of Patterns for Soft Human-Machine Interaction

Jinhyuk Lee
School of Electronic and Electrical Engineering
Kyungpook National University
Daegu, 41566, Korea
0920wlsgur@naver.com

Suwoong Lee
Department of Mechatronics
Technology Congergence Group
Korea Institute of Industrial Technology (KITECH)
Daegu, 42994, Korea
lee@kitech.re.kr

Min Young Kim*
School of Electronics Engineering
Kyungpook National University
Daegu, 41566, Korea
minykim@knu.ac.kr

***Abstract*— Tactile sensors are used in various fields such as automated factories and human collaboration. Tactile sensors exist in a variety of technological ways. In particular, most of the contact determination methods are mainly performed through the detection of the physical surface. In contrast, recently, various Vision-based tactile sensors that can replace the existing method based only on visual data from an image viewed through a camera sensor have been proposed. The hardware proposed in this paper is also a Vision-based tactile sensor, and it is a method that determines contact based only on patterns. In addition, we propose a vision-based tactile sensor as hardware in the form of air bag based on an air cushion. As the biggest feature of the Vision-based tactile sensor is estimation through image reading, it is easy to update various functions through algorithm improvement. Based on these points, through continuous research, we will develop algorithms for position estimation stability improvement, force estimation, and multi-touch discrimination, among at the possibility of application to fields such as cooperative human interaction robots.**

Keywords*— *Vision-based Tactile Sensor, image processing, air cushion, contact estimation

I. Introduction

Tactile sensor technology serves to detect the forces and pressures affected by the contact between the sensor and the object. In particular, with the advent of the era of the robot industry, it enables efficient and advanced work in work using robots, and is the most basic technology for performing all robot tasks. As such, tactile sensor technology has been applied and developed in various fields such as medical robots, industrial robot hands, and human interaction robots[1]. Correspondingly, various technological methods have also been developed. Representatively, there are resistive, capacitive, piezoelectric, optical, and vision technologies. Among the five technologies mentioned, they can be classified into two types: resistive, capacitive, piezoelectric and optical, and vision[2-6]. The big difference between these two classifications is that the former technology determines that a force is physically applied directly to the sensor, and the latter technology determines the change through the force applied to the surface by the sensor to be.

As such, the latter technique is advantageous in preventing aging and failure of the sensor since no direct force is applied to the sensor itself. In addition, since it is a method of judging through analysis of the changing amount of light or images, it has the advantage of enabling continuous technology updates in the future through algorithm development without reconfiguring the previously developed hardware configuration. For this reason, many studies have been conducted on vision-based tactile sensors. In addition, there are various design parts of the tactile sensor itself for determining contact. There are dome-shaped tactile sensor, air-filled tactile sensors, and light-changing tactile sensors[4-6,9].

In previous studies of vision-based tactile sensors, the main material is elastomer. A major feature of using elastomers is that the visual change on contact is prominent. In particular, many applications are made because the surface texture of a contacted object can also be well represented. In contrast, in this paper, we propose a vision-based tactile sensor that performs contact estimation by tracking the features of patterns extracted through image processing using a single camera vision sensor in the form of an air cushion through a specially manufactured material. Unlike elastomer, the characteristics of the proposed material are that external light is blocked and patterns of regular size and spacing are printed on the inside of the contact surface. In addition, unlike the existing vision-based tactile sensor, it is configured in the form of an air bag, so it is proposed to apply to another platform other than the robot hand tip part as a target.

II. Hardware configuration

The proposed hardware is a method in which the vision sensor that judges the contact and the change due to contact through air injection has a certain distance, and has the same shape as an air bag. The material is specially formulated and has some elasticity. The detailed configuration of the hardware is shown in Fig. 1 below.

(a)

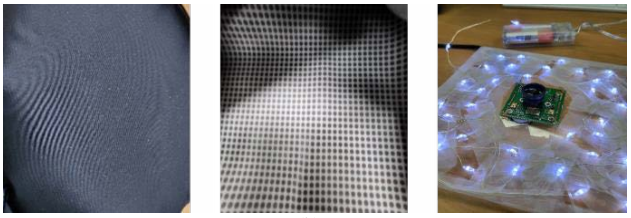

(b)

(c)

Fig. 1. Final hardware and internal configuration composed of air cushions.

(a) of Fig. 1 shows the vision-based tactile sensor hardware completed with an air cushion. When viewed from above, it has a diameter of about 30 cm in a circular shape, and when viewed from the side, it has a height of about 12 cm.

As can be seen in (b) of Fig. 1, the material of the air cushion is made of a blackout material that completely blocks external light, and a circular pattern is printed at the same size and interval on the inside of the contact part. Due to the characteristics of these materials, LEDs are used to supply light to the inside, and LEDs are placed around the vision sensor. In this way, an acrylic plate was used to fix the LED and the vision sensor, and the size of the connector of the cable to be connected for the operation of the vision sensor was processed on the acrylic plate so that it could be combined.

The rear part of the air cushion is shown in (c) of Fig 1, and for combining, the rear part of the blackout material with a pattern was cut and an acrylic plate with LED and vision sensor attached was inserted and combined. Since there is a difficulty in preventing air from leaking completely during the coupling process, a small air injection device was used to maintain the air, and continuous air retention was achieved through the coupling of the air injection unit.

III. Algorithm Configuration

The algorithm for contact estimation using the hardware configured above is shown as follows.

A. Image preprocessing and ID assignment

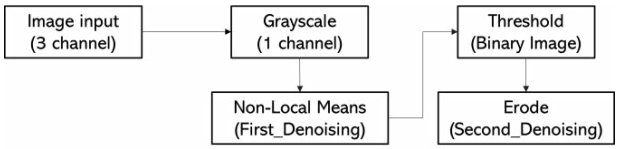

Fig. 2. Process of processing input images for pattern extraction.

From the input pattern image, first, the RGB 3-channel image is converted into a 1-channel grayscale image to reduce the amount of calculation in the processing to be performed. Then, in the converted grayscale image, NLMeans (Non-Local Means) Denoising Algorithm is applied to remove image noise while saving the details of the pattern in the video, and then binarization is performed to separate the pattern and the background[7].

Afterwards, the noise is once again removed by an erode process. Subsequently, a process of extracting contours of patterns from the binarized image and making each pattern traceable is performed.

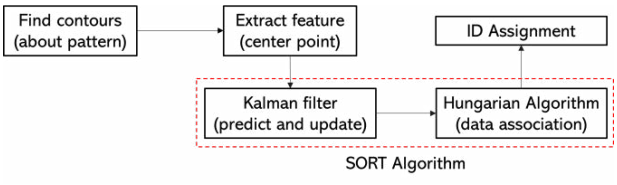

Fig. 3. The Process of extracting a pattern and making it a fixed ID.

The SORT algorithm is applied to make tracking possible for the center coordinates of the contour of the extracted pattern and to have a fixed ID[8]. The reason why this work is carried out is that the sequence of extracted patterns changes every time when the movement of the pattern occurs due to contact as the search proceeds sequentially from a specific direction in the general contour extraction method.

B. Contact position estimation

In order to estimate the location, a comparison criterion should be made from the previously processed id-given pattern. For this purpose, in this paper, the distance change amount, for each pattern is set as the standard. In order to have the distance change, first, all patterns have the average value of the distance values from 5 close-distance patterns through Euclidean distance calculation as the initial value for each pattern. This is because the size and shape of the patterns are not constant due to the characteristics of the random pattern, so there is difficulty in a simple comparison such as area comparison, and the distance between the patterns is also different. In addition, since it may be difficult to discriminate the change in spacing due to contact, it can be made in the form of a mesh as shown above to help in judging the change.

$$d = \sqrt{(x_1 - x_2)^2 + (y_1 - y_2)^2} \tag{1}$$

After that, when a change of more than a certain distance change occurs due to a change contact in real time based on the average distance value of the patterns at the beginning, the patterns from the pattern having the largest amount of change up to the fourth pattern are searched. Here, the patterns searched for are selected from those included within a certain range. Then, the average coordinate point for the four searched patterns is calculated as the first estimated point area. Since the estimated first point does not take into account how much each of the four patterns is actually affected by the change, the ratio is calculated in order to apply the influence of each of the four patterns. At this time, the ratio calculation is carried out by comparing the amount of change with each other and is calculated as follows, (2).

$$w_{1\cdots4} = \frac{\Delta d_{1\cdots4} \times 100}{\Delta d_1 + \Delta d_2 + \Delta d_3 + \Delta d_4} \tag{2}$$

The calculated ratio is applied to the difference value obtained through the difference between the coordinates of each of the four patterns and the average coordinates again as shown in below (3) and (4). After that, the final contact position is estimated by moving each applied difference value from the average coordinate to the direction of the pattern having the corresponding difference value.

$$xw_{1\cdots4} = \frac{\Delta x_{1\cdots4} w_{1\cdots4}}{100} \tag{3}$$

$$yw_{1\cdots4} = \frac{\Delta y_{1\cdots4} w_{1\cdots4}}{100} \tag{4}$$

C. Contact depth estimation

The depth value is also estimated through fitting to the actual depth value using the change value mentioned above. First, data on values that change according to the actual depth are collected. At this time, the collected data utilizes the change value of the pattern extracted by the occurrence of contact, and acquires values from several points to have the average value of the corresponding change value as the data to be fitted. The reason why the average value of the change value is used as the fitting data is that the patterns at the location where the contact occurs are not distributed equally but are distributed individually.

As a result, a pattern with a large amount of change is searched for, but among the searched patterns, a large difference occurs between the values of the maximum and minimum changes. Considering these points, the data are fitted with an average value. As the actual contact depth increases, the movement of the pattern occurs due to contact, and the distance value initially had is also proportional, and the value between the two increases equally. Focusing on these points, we proceed with an optimized fitting so that the characteristics of the data can be well represented at the same time as analysis.

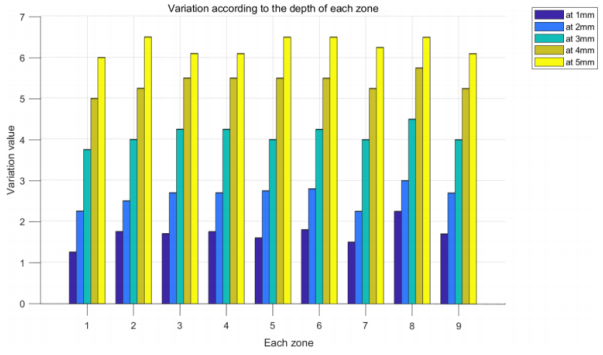

Fig. 4. The change value according to the depth of eachzone.

Based on the data obtained as shown in Fig. 4, fitting is performed as shown in Fig. 5. And then, By appropriately adjusting the degree of the polynomial, the final coefficient of the 3rd degree polynomial was obtained by determining the suitability of the actual depth value and the change value, and finally, the depth estimation formula was derived as shown in (5) below.

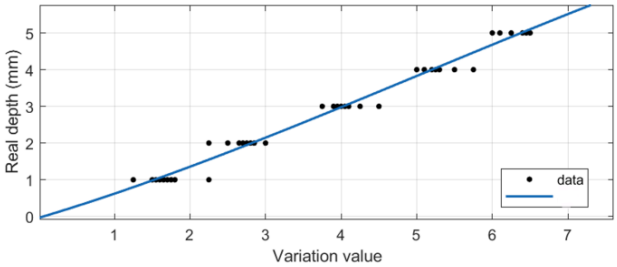

Fig. 5. The results of fitting based on the acquired data.

$$z_{est} = -0.003112(\Delta d_{avg})^3 + 0.0473(\Delta d_{avg})^2 + 0.6143\Delta d_{avg} - 0.03689 \quad (5)$$

IV. Experiments

For the experiment on the proposed algorithm, it is applied to self-made vision-based tactile sensors, and the sensor is evaluated through a jig. The jig used can be operated in units of 1 mm in each of the x, y, and z-axis directions. At the bottom, vision-based tactile sensors is fixed to configure the experimental environment, and then the actual position of the jig and the position estimated by contact are compared. In this way, accuracy, error rate, and precision are measured.

Fig. 6. Test environment for vision-based tactile sensor.

First, Fig. 4 shows the contact estimation result of the vision-based tactile sensor composed of the second hardware, the air cushion.

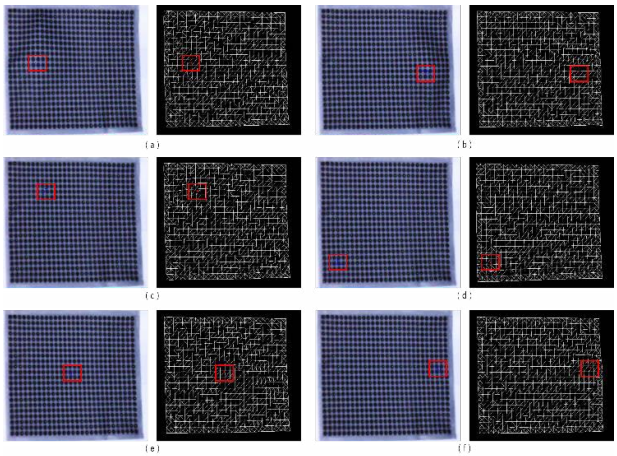

Fig. 7. The result of estimation due to contact in composed vision-based tactile sensor. (Left images: acquired camera images, Right images: estimated positions using the proposed algorithms)

Here, each image on the left represents an image seen by a vision sensor as an actual contact. In addition, each image on the right is a contact estimation result shown in a virtual image showing how the final contact is estimated in a state in which all patterns are connected to each other and formed in a mesh form through the application of the proposed algorithm.

For the entire experiment, the proposed algorithm was applied to conduct repeated experiments by depth for a total of 10 zones on the contact surface, and some of the evaluation results through the contact judgment experiment are shown in Table 1.

TABLE I. PART OF THE CONTACT ESTIMATION EXPERIMENT RESULTS

	Actual contact coordinates			X, Y	Z	Estimated contact coordinates			Error		
	X	Y	Z	cm	mm	X	Y	z	X	Y	Z
	(PIX)	(PIX)	(mm)	Jig movement distance		(PIX)	(PIX)	(mm)	(PIX)	(PIX)	(mm)
A	275	200	2	-1/0	2	273	203	1.9	2	3	0.1
				-1/0	2	278	205	2	3	5	0
				-1/0	2	268	197	2	7	3	0
				-1/0	2	273	203	1.9	2	3	0.1
				-1/0	2	268	203	2.1	7	3	0.1
B	375	250	3	+1/0	3	375	257	3	0	7	0
				+1/0	3	373	256	3.1	2	6	0.1
				+1/0	3	369	257	3.1	6	7	0.1
				+1/0	3	369	254	3	6	4	0
				+1/0	3	369	257	2.9	6	7	0.1
C	360	175	2	0/-1	2	360	176	1.9	0	1	0.1
				0/-1	2	353	182	2	7	7	0
				0/-1	2	361	171	1.9	1	4	0.1
				0/-1	2	358	171	1.8	2	4	0.2
				0/-1	2	352	181	2	8	6	0
D	285	260	3	0/+1	3	275	266	2.9	10	6	0.1
				0/+1	3	281	261	3	4	1	0
				0/+1	3	286	256	2.9	1	4	0.1
				0/+1	3	289	266	2.9	4	6	0.1
				0/+1	3	290	261	3	5	1	0
E	210	160	2	-2/0	2	219	164	2.2	9	4	0.2
				-2/0	2	214	157	2.3	4	3	0.3
				-2/0	2	219	161	2.1	9	1	0.1
				-2/0	2	218	164	2	8	4	0
				-2/0	2	218	161	2.1	8	1	0.1

The maximum error pixels of the X and Y coordinates are 10 pixels and 7 pixels, respectively, showing a larger error than the minimum error. However, the total error averages of the X and Y coordinates are 4.84 pixels and 4.04 pixels, showing values between about 4 and 5 pixels. The Z-axis, which is the depth, also shows a larger error than the minimum error with the maximum error being 0.3 mm, but the overall error average shows a value of 0.08 mm.

V. CONCLUSION

The vision-based tactile sensor made of the air cushion proposed in this paper uses the vision sensor and pattern to determine contact. The proposed tactile sensor also has an advantage in preventing aging of the vision sensor as the contact is not directly applied to the vision sensor, and it is easy to add functionality through algorithm development as it reads the contact through an image.

Table 2 below shows the accuracy, error rate, and precision through the final experiment. As can be seen in the table, when the proposed algorithm is applied to an air cushion with a regular pattern, the contact estimation results for x, y, and z show accuracy and error rate close to the actual contact value. However, it can be confirmed that the estimation error rate for z is relatively high, unlike x and y. Unlike the unit of x and y being pixel, z is evaluated in mm unit, and it seems that the same level of results are not derived. Nonetheless, the z estimation also shows satisfactory results.

TABLE II. FINAL RESULTS OF THE EXPERIMENT

		Estimation result of vision-based tactile sensor made of air cushion through application of proposed algorithm
Accuracy	X	98.76 %
	Y	98.52 %
	Z	97.38 %
Error rate	X	1.372 %
	Y	1.86 %
	Z	3.236 %
Precision	X	2.73 pixel
	Y	2.84 pixel
	Z	0.075 mm

However, the proposed vision-based tactile sensor has limitations in estimating the maximum depth due to the constraint that the contact patterns must be changed within the vision sensor's field of view and the hardware design characteristics. In particular, in this paper, experiments were conducted using jig tips of the same size, but unlike the tips used, there is a disadvantage that inaccurate results may be obtained in estimation depending on the size of the object to be actually contacted. In order to compensate for this problem, if the partial shape of the object in the contacted area can be estimated, it is judged that more accurate contact estimation can be made regardless of the size of the object to be contacted, and additional research is needed.

In the future, by improving the accuracy of position estimation, we will proceed with research on multi-touch estimation and algorithms capable of force estimation based on higher accuracy estimation results. In addition, as part of soft robotics, it is expected to perform the role of nursing for the elderly and patients in the coexistence system of humans and robots by using humanoid robots as body parts or applying health care equipment.

ACKNOWLEDGMENT

This work was supported by the National Research Foundation of Korea (NRF) grant funded by the Korea government (MSIT) (No. 2022R1A2C2008133). And This research was also supported by the Basic Science Research Program through the National Research Foundation of Korea (NRF), funded by the Ministry of Education (2021R1A6A1A03043144). Also This research has been conducted with the support of the Korea Institute of Industrial Technology (KITECH) as "Development of Soft Robotics Technology for Human-Robot Coexistence Care Robots (EH-22-0002)"

REFERENCES

[1] J. Tegin and J. Wikander, "Tactile sensing in intelligent robotic manipulation – a review," Industrial Robot, Vol. 32, no. 1, pp. 64-70, Feb. 2005

[2] K. Shimonomura, "Tactile image sensors employing camera: A review," Sensors, Vol. 19, no. 18, p. 3933, Sep. 2019

[3] U.H. Shah, R. Muthusamy, D. Gan, et al., "On the Design and Development of Vision-based Tactile Sensors," Journal of Intelligent & Robotic Systems, Vol. 102, no. 82, Jul. 2021

[4] W. Yuan, S. Dong, E.H. Adelson, "Gelsight: High-resolution robot tactile sensors for estimating geometry and force," Sensors, Vol. 17, no. 12, p. 2762, Nov. 2017

[5] M. Lambeta et al., "DIGIT: A Novel Design for a Low-Cost Compact High-Resolution Tactile Sensor With Application to In-Hand Manipulation," in IEEE Robotics and Automation Letters, Vol. 5, no. 3, pp. 3838-3845, Jul. 2020

[6] N. Kuppuswamy, A. Alspach, A. Uttamchandani, S. Creasey, T. Ikeda and R. Tedrake, "Soft-bubble grippers for robust and perceptive manipulation," 2020 IEEE/RSJ International Conference on Intelligent Robots and Systems(IROS), PP. 9917-9924, Oct. 2020

[7] A. Buades, B. Coll and J.-M. Morel, "A non-local algorithm for image denoising," 2005 IEEE Computer Society Conference on Computer Vision and Pattern Recognition(CVPR'05), Vol. 2, pp. 60-65, Jun. 2005

[8] A. Bewley, Z. Ge, L. Ott, F. Ramos and B. Upcroft, "Simple Online and Realtime Tracking," 2016 IEEE International Conference on Image Processing(ICIP), pp. 3464-3468, Sep. 2016

[9] J. Lee, S. Lee, H. M. Oh, B. R. Cho, K. -H. Seo, and M. Y. Kim, "3D Contact Position Estimation of Image Sensors," Sensors, Vol. 20, no. 13, p. 3796, Jul. 2020